IX CONGRESSO BRASILEIRO DE
ENGENHARIA E CIÊNCIAS TÉRMICAS
9th BRAZILIAN CONGRESS OF THERMAL
ENGINEERING AND SCIENCES

Paper CIT02-0106

NUMERICAL SIMULATION OF TURBULENT FREE-SURFACE FLOWS

V. G. Ferreira
Departamento de Estatística, Matemática Aplicada e Computação, Instituto de Geociências e Ciências Exatas, Av. 24-A, 1515 - C.P. 178 - 13500-230, Rio Claro, SP, Brazil
e-mail, pvgf@lcad.icmc.sc.usp.br

N. Mangiavacchi
Departamento de Ciências de Computação e Estatística, Instituto de Ciências Matemáticas e de Computação, Av. Trabalhador São Carlense, 400, C.P. 668, 13251-900, São Carlos, SP, Brazil
e-mail, norberto@lcad.icmc.sc.usp.br

M. F. Tomé
Departamento de Ciências de Computação e Estatística, Instituto de Ciências Matemáticas e de Computação, Av. Trabalhador São Carlense, 400, C.P. 668, 13251-900, São Carlos, SP, Brazil
e-mail, murilo@lcad.icmc.sc.usp.br

J. A. Cuminato
Departamento de Ciências de Computação e Estatística, Instituto de Ciências Matemáticas e de Computação, Av. Trabalhador São Carlense, 400, C.P. 668, 13251-900, São Carlos, SP, Brazil
e-mail, jacumina@lcad.icmc.sc.usp.br

A. Castelo
Departamento de Ciências de Computação e Estatística, Instituto de Ciências Matemáticas e de Computação, Av. Trabalhador São Carlense, 400, C.P. 668, 13251-900, São Carlos, SP, Brazil
e-mail, castelo@lcad.icmc.sc.usp.br

S. McKee
Department of Mathematics, University of Strathclyde, Livingstone Tower, 26 Richmond Street, Glasgow, G1 1XH, Scotland, UK
e-mail, caas29@maths.strath.ac.uk

Abstract. *This paper presents numerical simulations of incompressible turbulent free-surface fluid flow problems. The methodology employed to solve the Reynolds Averaged Navier-Stokes equations and $\kappa - \varepsilon$ turbulence equations is an extension of GENSMAC: a finite-difference marker-and-cell technique for the numerical solution of incompressible free-surface flows using a velocity-pressure formulation. The numerical solution procedure is applied to a turbulent boundary-layer on a flat plate and a jet impinging onto a flat surface.*

Keywords: *turbulent fluid flow, Reynolds Averaged Navier-Stokes, free-surface fluid flow, finite-difference formulation, $\kappa - \varepsilon$ turbulence model*

1. Introduction

In the two-dimensional cartesian coordinate system, the governing equations for incompressible turbulent fluid flows are the Reynolds Averaged Navier-Stokes (RANS) equations

$$\frac{\partial u}{\partial t}+\frac{\partial (uu)}{\partial x}+\frac{\partial (uv)}{\partial y}=-\frac{\partial p_e}{\partial x}+\frac{1}{Re}\frac{\partial}{\partial y}\left(\frac{\partial u}{\partial y}-\frac{\partial v}{\partial x}\right)+\frac{1}{Fr^2}g_x+\frac{1}{Re}\left[2\frac{\partial}{\partial x}\left(\nu_t\frac{\partial u}{\partial x}\right)+\frac{\partial}{\partial y}\left(\nu_t\left(\frac{\partial u}{\partial y}+\frac{\partial v}{\partial x}\right)\right)\right], \quad (1)$$

$$\frac{\partial v}{\partial t}+\frac{\partial (vu)}{\partial x}+\frac{\partial (vv)}{\partial y}=-\frac{\partial p_e}{\partial y}-\frac{1}{Re}\frac{\partial}{\partial x}\left(\frac{\partial u}{\partial y}-\frac{\partial v}{\partial x}\right)+\frac{1}{Fr^2}g_y+\frac{1}{Re}\left[2\frac{\partial}{\partial y}\left(\nu_t\frac{\partial v}{\partial y}\right)+\frac{\partial}{\partial x}\left(\nu_t\left(\frac{\partial u}{\partial y}+\frac{\partial v}{\partial x}\right)\right)\right], \quad (2)$$

$$\frac{\partial u}{\partial x}+\frac{\partial v}{\partial y}=0, \quad (3)$$

where t is the time, $u = u(x, y, t)$ and $v = v(x, y, t)$ are, respectively, the components in the x and y directions of the local time-averaged velocity vector field $\mathbf{u} = \mathbf{u}(x, y, t)$, $p_e = p + \frac{2}{3}\frac{1}{Re}\kappa$ is the effective pressure, being

$\kappa = \kappa(x,y,t)$ the time-averaged turbulent kinetic energy, ν is the kinematic viscosity of the fluid, and ν_t is the eddy-viscosity. The non-dimensional parameters $Re = U_0 L_0/\nu$ and $Fr = U_0/\sqrt{L_0|\mathbf{g}|}$ denote the associated Reynolds and Froude numbers, respectively, in which U_0 is a characteristic velocity scale and L_0 is a length scale. Equations (1) through (3) form a closed system, which can be solved for the variables u, v and p_e, provided that an acceptable turbulent model is defined.

In this work, the closure of the RANS equations is made by using two-equation $\kappa - \varepsilon$ turbulence models

$$\frac{\partial \kappa}{\partial t} + \frac{\partial (u\kappa)}{\partial x} + \frac{\partial (v\kappa)}{\partial y} = \frac{1}{Re}\left[\frac{\partial}{\partial x}\left((1+\nu_t/\sigma_\kappa)\frac{\partial \kappa}{\partial x}\right) + \frac{\partial}{\partial y}\left((1+\nu_t/\sigma_\kappa)\frac{\partial \kappa}{\partial y}\right)\right] + P - \varepsilon, \tag{4}$$

$$\frac{\partial \varepsilon}{\partial t} + \frac{\partial (u\varepsilon)}{\partial x} + \frac{\partial (v\varepsilon)}{\partial y} = \frac{1}{Re}\left[\frac{\partial}{\partial x}\left((1+\nu_t/\sigma_\varepsilon)\frac{\partial \varepsilon}{\partial x}\right) + \frac{\partial}{\partial y}\left((1+\nu_t/\sigma_\varepsilon)\frac{\partial \varepsilon}{\partial y}\right)\right] + (C_{1\varepsilon}P - C_{2\varepsilon}\varepsilon)/T_t + \beta E, \tag{5}$$

where $\varepsilon = \varepsilon(x,y,t)$ is the dissipation rate of κ, and C_μ, $C_{1\varepsilon}$, $C_{2\varepsilon}$, σ_κ and σ_ε are empirical constants. The isotropic eddy-viscosity, the production of turbulence P, the source term E and the turbulence time scale T_t are, respectively, defined as

$$\nu_t = C_\mu f_\mu \kappa T_t, \tag{6}$$

$$P = \nu_t \left(2\left(\frac{\partial u}{\partial x}\right)^2 + 2\left(\frac{\partial v}{\partial y}\right)^2 + \left(\frac{\partial v}{\partial x} + \frac{\partial u}{\partial y}\right)^2\right), \tag{7}$$

$$E = \frac{2\nu_t}{Re}\left(\left(\frac{\partial^2 v}{\partial x^2}\right)^2 + \left(\frac{\partial^2 u}{\partial y^2}\right)^2\right), \tag{8}$$

$$T_t = (1-\beta)Min\left\{\frac{\kappa}{\varepsilon}, \frac{2}{3C_\mu}\sqrt{\frac{3}{8|\mathbf{S}|^2}}\right\} + \beta\left\{\frac{\kappa}{\varepsilon} + \left(\frac{1}{\varepsilon}\right)^{1/2}\right\}, \tag{9}$$

where, in Eq. (9), $|\mathbf{S}|^2 = \mathbf{D}:\mathbf{D}$, with $\mathbf{D} = \nabla\mathbf{u} + (\nabla\mathbf{u})^{\mathbf{T}}$. Together with the model constants, the parameter β appearing in Eqs. (5) and (9) is used to specify the $\kappa - \varepsilon$ model. In the case of $C_\mu = 0.09$, $C_{1\varepsilon} = 1.44$, $C_{2\varepsilon} = 1.92$, $\sigma_\kappa = 1.0$, $\sigma_\varepsilon = 1.3$ and $\beta = 0$, we deal with the high-Reynolds $\kappa - \varepsilon$ model of Launder and Spalding, 1974 (HRe $\kappa - \varepsilon$ model), with the time scale proposed by Durbin, 1996 for appropriated treatment of stagnation-point anomaly. When the model constants are that proposed by Hoffman, 1975; that is, $C_\mu = 0.09$, $C_{1\varepsilon} = 1.81$, $C_{2\varepsilon} = 2.0$, $\sigma_\kappa = 2.0$, $\sigma_\varepsilon = 3.0$ and $\beta = 1$, we treat with a low-Reynolds $\kappa - \varepsilon$ model (LRe $\kappa - \varepsilon$ model), similar to that proposed by Yang and Shih, 1993. The dependent variables in Eqs. (1)-(9) have been nondimensionalized by U_0, L_0 and ν in the usual way. The damping function f_μ in Eq. (6) assumes the value $f_\mu = 1$ in the case of the HRe $\kappa - \varepsilon$ model, and takes the following expression in the case of the LRe $\kappa - \varepsilon$ model

$$f_\mu = \left(1 - Exp(-a_1 Re_{y_w} - a_3 Re_{y_w}^3 - a_5 Re_{y_w}^5)\right)^{1/2}, \tag{10}$$

where a_1, a_3 and a_5 are constants given by

$$a_1 = 1.5 \times 10^{-4}, a_3 = 5.0 \times 10^{-7}, a_5 = 1.0 \times 10^{-10}, \tag{11}$$

and Re_{y_w} is the local Reynolds number defined by

$$Re_{y_w} = y_w Re \kappa^{1/2}, \tag{12}$$

being y_w the normal distance from the rigid-boundary to a point into the flow.

The main purpose of this work is to present numerical simulations of incompressible turbulent free-surface fluid flow problems using the HRe $\kappa - \varepsilon$ and LRe $\kappa - \varepsilon$ turbulence models. The numerical solution procedure is applied to a turbulent boundary-layer on a flat plate and a jet impinging onto a flat surface.

2. Initial and Boundary Conditions

Equations (1) through (5) are coupled, non-linear, partial differential equations and, together with the eddy-viscosity model (6), are sufficient, in principle, to solve for the five unknowns u, v, p_e, κ and ε when appropriated initial and boundary conditions are specified. In this work, a staggered grid is used where the effective pressure, the turbulent kinetic energy and the dissipation rate are stored at the center of a computational cell, whereas velocities are stored at the cell boundaries. With this grid system, effective pressure boundary conditions are not needed.

For initial conditions, the values of all variables are prescribed. Five types of boundary conditions are used, namely: inflow, outflow, symmetry, free-surface, and rigid-wall boundaries. At the inflow, the values of u, v, κ and ε are prescribed. At the outflow, the streamwise gradient for each variable is required to be equal to zero. At symmetry boundaries, we are using

$$u_n = 0, \quad \frac{\partial u_t}{\partial n} = 0, \quad \frac{\partial \kappa}{\partial n} = 0 \quad \text{and} \quad \frac{\partial \varepsilon}{\partial n} = 0, \tag{13}$$

where n and t denote normal and tangential directions to the boundary, respectively. At the free-surface, we are considering that the fluid is moving into a passive atmosphere (zero-pressure) and, in the absence of surface tension forces, the normal and tangential components of the stress must be continuous across any free-surface, so that on such a surface we have (see, for example, Ladau and Lifshitz, 1987)

$$\mathbf{n} \cdot (\sigma \cdot \mathbf{n}) = 0, \tag{14}$$

$$\mathbf{m} \cdot (\sigma \cdot \mathbf{n}) = 0. \tag{15}$$

In the above equations, $\mathbf{n}$ and $\mathbf{m}$ are unit normal and tangent vectors to the surface, and σ is the general constitutive equation (Cauchy stress-tensor) defined as

$$\sigma = -p_e \, \mathbf{I} + \frac{1}{Re}(1 + \nu_t)\mathbf{D}, \tag{16}$$

where $\mathbf{I}$ denotes the identity tensor. From Eqs. (14) and (15), we determine the effective pressure and the velocities, respectively. The turbulent variables at the free-surface are determined by imposing

$$\frac{\partial \kappa}{\partial n} = 0 \quad \text{and} \quad \frac{\partial \varepsilon}{\partial n} = 0. \tag{17}$$

The boundary conditions at rigid-wall depend on the $\kappa - \varepsilon$ model considered. When the simulation is performed with the HRe $\kappa - \varepsilon$ model, the wall-function approach (Launder and Spalding, 1974) is used. In this case, the fundamental equation for determining the fictitious velocities and turbulent variables near a rigid-wall is the total wall shear stress τ_w given by

$$\frac{1}{Re}(1 + \nu_t)\left|\frac{\partial \hat{u}}{\partial n}\right| \approx {u_\tau}^2 = \tau_w, \tag{18}$$

where $\hat{u}$ represents the velocity component tangential to the rigid-wall, and u_τ is the friction velocity. The values of the κ and ε in the inertial sublayer are given by

$$\kappa = Re\frac{\tau_w}{C_\mu^{1/2}} \quad \text{and} \quad \varepsilon = Re\frac{\tau_w u_\tau}{K y_w}, \tag{19}$$

being $K = 0.41$ the von Kármán constant. In the viscous sublayer, we are using the strategy of Sondak and Pletcher, 1995, that is,

$$\kappa = Re\frac{\tau_w}{C_\mu^{1/2}}\left(\frac{y^+}{{y_c}^+}\right)^2 \quad \text{and} \quad \varepsilon = \sqrt{\frac{1}{Re}}\frac{\kappa^{3/2}}{l^*}, \tag{20}$$

where y^+ is defined as $y^+ = Re u_\tau y_w$ and l^* represents the length scale proposed by Norris and Reynolds, 1975. Neglecting the buffer layer of a turbulent boundary-layer, the critic y^+ (${y_c}^+$) in Eq. (20) delimits the viscous sublayer and the inertial sublayer. A detailed discussion of the initial and boundary conditions using the HRe $\kappa - \varepsilon$ turbulence model is given in Ferreira, 2001. When the LRe $\kappa - \varepsilon$ model is used in the simulations, the velocity at solid boundary is set to zero, in order to represent the no-slip condition ($\mathbf{u} = \mathbf{0}$), and the values of the variables κ and ε at this boundary are

$$\kappa = 0 \quad \text{and} \quad \varepsilon = \frac{2}{Re}\left(\frac{\partial \kappa^{1/2}}{\partial n}\right)^2. \tag{21}$$

2.1. Wall-Function Aspects

It is well known that the HRe $\kappa - \varepsilon$ model requires modification for the simulation of flow near rigid boundaries, so as to account for damping of velocity flutuations and viscous effects. In general, the solution of the conservation equations in the inner layer is not necessary since the flow mechanism in such a region can be described reasonably well by employing wall-functions (for a more datailed discussion see, for example, Ferreira,

2001). The behavior of the mean velocity profiles in the viscous and inertial sublayers are, respectively, given by (see, for example, Bradshaw, 1976, Wilcox, 1988, or White, 1991)

$$u^+ - y^+ = 0, \tag{22}$$

$$ln(Ey^+) - Ku^+ = 0, \tag{23}$$

where $u^+ = \hat{u}/u_\tau$ and $E = exp(K5.1)$.

One of the central questions in the application of the wall-functions (18)-(20) is the determination of the friction velocity, and hence the wall shear stress. It is determined from relation (22) or (23), depending on the local Reynolds number y^+. When u_τ is obtained by (23), the Newton-Raphson's method is applied with $u_\tau = 11.60$ as the initial condition. We initiate the calculations by determining the critic Reynolds number ${y_c}^+$, solution of the non-linear equation defined by the intersection of (22) and (23), and by imposing that it is in the viscous sublayer. By neglecting the transition sublayer, in every cycle of the computational procedure, the friction velocity is estimated in the following manner: with the tangential velocity $\hat{u}$ known in the first cell adjacent to the wall, u_τ is apdated according to the value of the y^+ given by (22). If y^+ is less than ${y_c}^+$, we use (22); on the other hand, we employ (23). The fictitious velocities are calculated by central-diference aproximation of the Eq. (18).

3. Solution Procedure

The governing equations (1) through (5) are solved with an extension of the GENSMAC methodology for turbulent flow field (see Ferreira, 2001). The detailed information of the GENSMAC for the simulation of free-surface flows without turbulence modelling is provided in Tomé and McKee, 1994 and Tomé et al., 2000. It is a finite-difference, explicit, first/second-order accurate numerical method based on a predictor-corrector scheme. By using a guessed effective pressure $\tilde{p}_e$ and an eddy-viscosity ν_t, the method consists of solving the time-averaged Navier-Stokes equations (1)-(2) at the $(k+1)$ time-step for a tentative velocity field $\tilde{\mathbf{u}}$. The $\tilde{\mathbf{u}}$ is related to the true velocity field $\mathbf{u}$, at the $(k+1)$ time-step, by an auxiliary potential function ψ which is calculated by a Poisson equation, originated by imposing $\nabla \cdot \mathbf{u} = 0$ at the $(k+1)$ time-step. The effective pressure and the turbulent variables κ and ε are then updated, and the procedure is repeated at each time-step. In particular, when calculating $\tilde{\mathbf{u}}$ in step 1, we employ an adaptive time-stepping routine (see Tomé and McKee, 1994). The numerical solution procedure may be summarized as follows.

It is supposed that, at a given time $t = t_0$, the velocity field $\mathbf{u}$ is known and suitable boundary conditions for the velocity and turbulent variables are given. Let $\tilde{p}_e(x, y, t)$ be an arbitrary effective pressure field, which satisfies the correct pressure condition on the free-surface. This pressure field is constructed by employing the normal-stress condition (14) at the free-surface, and it is chosen arbitrarily (for instance $\tilde{p}_e(x, y, t) = 0$) into the fluid. The updated velocity field, the effective pressure and the turbulent variables, at time $t = t_0 + \delta t$, are calculated by the following steps:

1. With the eddy-viscosity ν_t known at $t = t_0$, compute an approximate velocity field $\tilde{\mathbf{u}}(x, y, t)$ from a finite-diference discretization of

$$\left.\frac{\partial \widetilde{u}}{\partial t}\right|_{t=t_0} = \left\{ -\frac{\partial(uu)}{\partial x} - \frac{\partial(uv)}{\partial y} - \frac{\partial \widetilde{p}_e}{\partial x} + \frac{1}{Re}\frac{\partial}{\partial y}\left(\frac{\partial u}{\partial y} - \frac{\partial v}{\partial x}\right) + \frac{1}{Fr^2}g_x \right.$$

$$\left. + \frac{1}{Re}\left[2\frac{\partial}{\partial x}\left(\nu_t \frac{\partial u}{\partial x}\right) + \frac{\partial}{\partial y}\left(\nu_t\left(\frac{\partial u}{\partial y} + \frac{\partial v}{\partial x}\right)\right)\right] \right\}\Bigg|_{t=t_0}, \tag{24}$$

$$\left.\frac{\partial \widetilde{v}}{\partial t}\right|_{t=t_0} = \left\{ -\frac{\partial(vu)}{\partial x} - \frac{\partial(vv)}{\partial y} - \frac{\partial \widetilde{p}_e}{\partial y} - \frac{1}{Re}\frac{\partial}{\partial x}\left(\frac{\partial u}{\partial y} - \frac{\partial v}{\partial x}\right) + \frac{1}{Fr^2}g_y \right.$$

$$\left. + \frac{1}{Re}\left[2\frac{\partial}{\partial y}\left(\nu_t \frac{\partial v}{\partial y}\right) + \frac{\partial}{\partial x}\left(\nu_t\left(\frac{\partial u}{\partial y} + \frac{\partial v}{\partial x}\right)\right)\right] \right\}\Bigg|_{t=t_0}, \tag{25}$$

with $\tilde{\mathbf{u}}(x, y, t_0) = \mathbf{u}(x, y, t_0)$ using the correct boundary conditions for $\mathbf{u}(x, y, t_0)$. It can be shown (see, for example, Ferreira, 2001) that $\tilde{\mathbf{u}}(x, y, t)$ possesses the correct vorticity at time t but does not satisfy (3), in general. By writting

$$\mathbf{u}(x, y, t) = \tilde{\mathbf{u}}(x, y, t) - \nabla\psi(x, y, t) \tag{26}$$

and imposing

$$\nabla^2\psi(x,y,t) = \nabla \cdot \tilde{\mathbf{u}}(x,y,t), \tag{27}$$

a velocity field is obtained in which the vorticity and mass are conserved;

2. Solve the Poisson equation (27) for ψ. The appropriate boundary conditions for this elliptic equation are homogeneous Dirichlet-type on the free-surface and homogeneous Neumann-type on fixed boundaries. These are treated in a similar way as in the GENSMAC codes of Tomé and McKee, 1994 and Tomé et al., 2000;
3. Calculate the velocity field $\mathbf{u}(x,y,t)$ from (26);
4. Compute the effective pressure. It can be shown (see Ferreira, 2001) that the effective pressure field is given by

$$p_e(x,y,t) = \tilde{p}_e(x,y,t) + \psi(x,y,t)/\delta t; \tag{28}$$

5. Compute the kinetic energy κ from a finite-difference approximation of (4);
6. Compute the dissipation rate ε from a finite-difference approximation of (5);
7. Update the eddy-viscosity ν_t from (6);
8. Particle movement. The last step in the calculation involves the movement of the marker particles to their new positions. These are virtual particles (without mass, volume, or other properties), whose coordinates are stored and updated at the end of each cycle by solving the ordinary differential equations

$$\frac{dx}{dt} = u \quad \text{and} \quad \frac{dy}{dt} = v \tag{29}$$

by Euler's method. This provides a particle with its new coordinates, allowing us to determine whether or not it has moved into a new computational cell, or if it has left the containment region through an outflow-boundary;

9. Update the boundary conditions and go back to the first step.

4. Discretization

In the solution procedure outlined above, the differential equations are discretized in time and space in precisely the same manner for all dependent variables. The temporal derivatives are discretized using the first-order forward difference (Euler's method), while the spatial derivatives are evaluated using specific finite-differences on a uniform staggered grid system. The convection terms are approximated by the high-order oscillation-free upwinding VONOS scheme of Varonos and Bergeles, 1998, which satisfy the Convection Boundedness Criterion (CBC) formulated by Gaskell and Lau, 1988. A detailed discussion of high-order convection schemes, including the VONOS one, would go beyond the scope of this paper, and the reader is referred to Ferreira et al., 2002 for details of the implementation and application. All the other derivatives are approximated using standard second-order central-difference formulation. The Poisson equation (27) is discretized using the usual five-point Laplacian operator, and the corresponding symmetric-positive definite linear system is solved by the conjugate-gradient method.

5. Numerical Results

First, results with the HRe $\kappa-\varepsilon$ model will be presented for the turbulent boundary-layer on a flat plate. For this problem, the Reynolds number based on the inflow velocity $U_0 = 1.0$ m/s and the channel height $H = 1.0$ m is $Re = 2.0 \times 10^6$. Three different meshes are used: a coarse mesh (20×100 computational cells, $\delta x = \delta y = 0.05$ m); a medium mesh (40×200 computational cells, $\delta x = \delta y = 0.025$ m); and a fine mesh (80×400 computational cells, $\delta x = \delta y = 0.0125$ m). Figure 1 shows a comparison between the turbulent skin-friction coefficient profiles C_f, as a function of the $Re_x = U_0 x/\nu$, obtained by the HRe $\kappa-\varepsilon$ model, in the three meshes and at the adimensional time $t = 6.477$, and the estimates given by Prandtl, power-law and White (see, for example, White, 1991). In this figure, for simple comparison, the theoretical profile for laminar flow field is also presented. As shown in Figs. 1 a), b) and c), the numerical estimates are generally satisfactory for Re_x beyond 1.0×10^6. It can also be observed from Fig. 1 d) that when the coarse mesh is twice refined, there was convergence of the numerical solution for a profile near the power-law and White profiles. On the other hand,

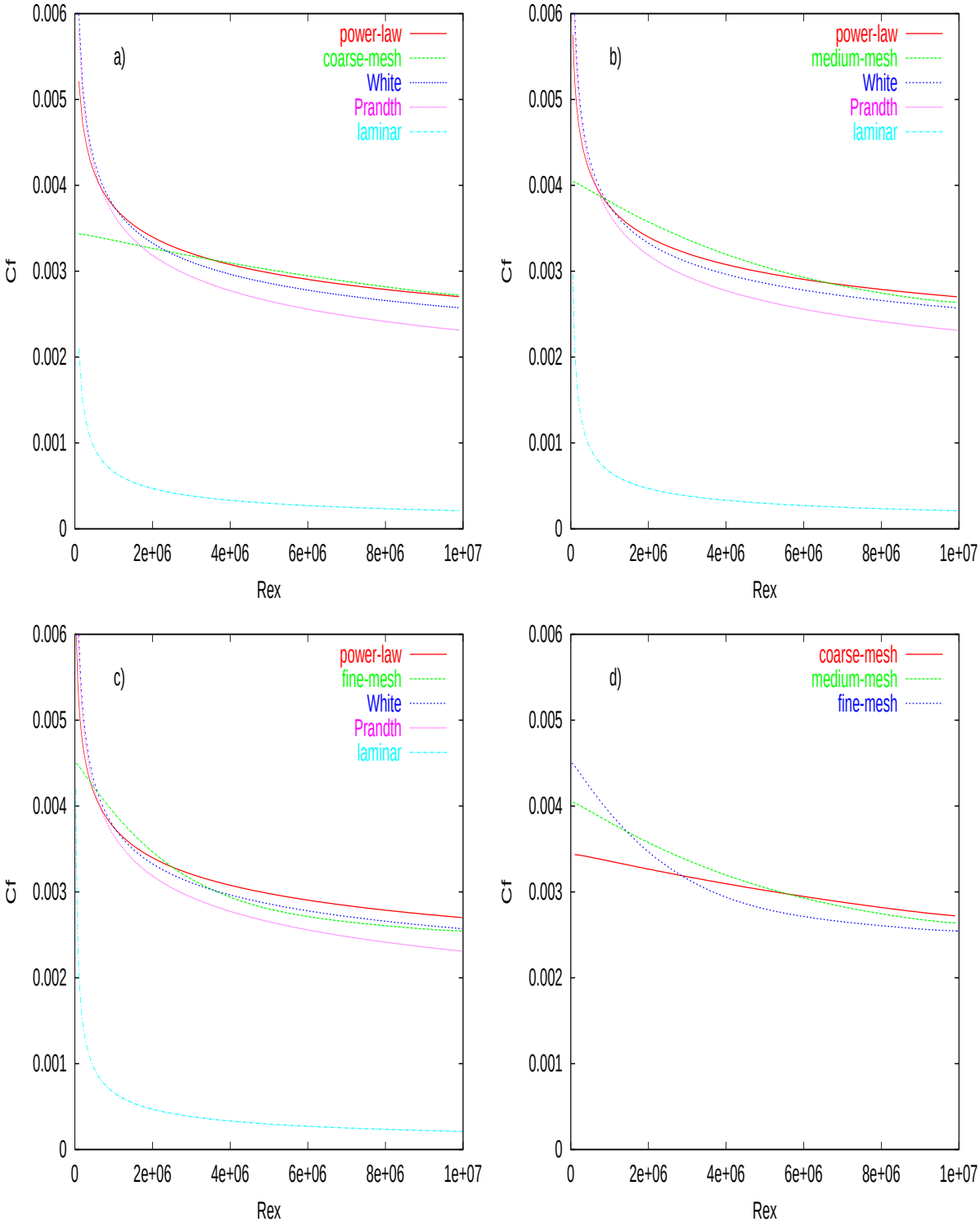

Figure 1: Comparison between the skin-friction coefficient profiles $C_f = C_f(Re_x)$ for the turbulent boundary-layer on a flat plate, showing well known theoretical estimates and that by HRe $\kappa - \varepsilon$ model: **a)** Comparison in the coarse mesh; **b)** Comparison in the medium mesh; **c)** Comparison in the fine mesh; **c)** Comparison of the three numerical solutions in the three meshes. $C_f = 2\tau_w/\rho {U_0}^2$.

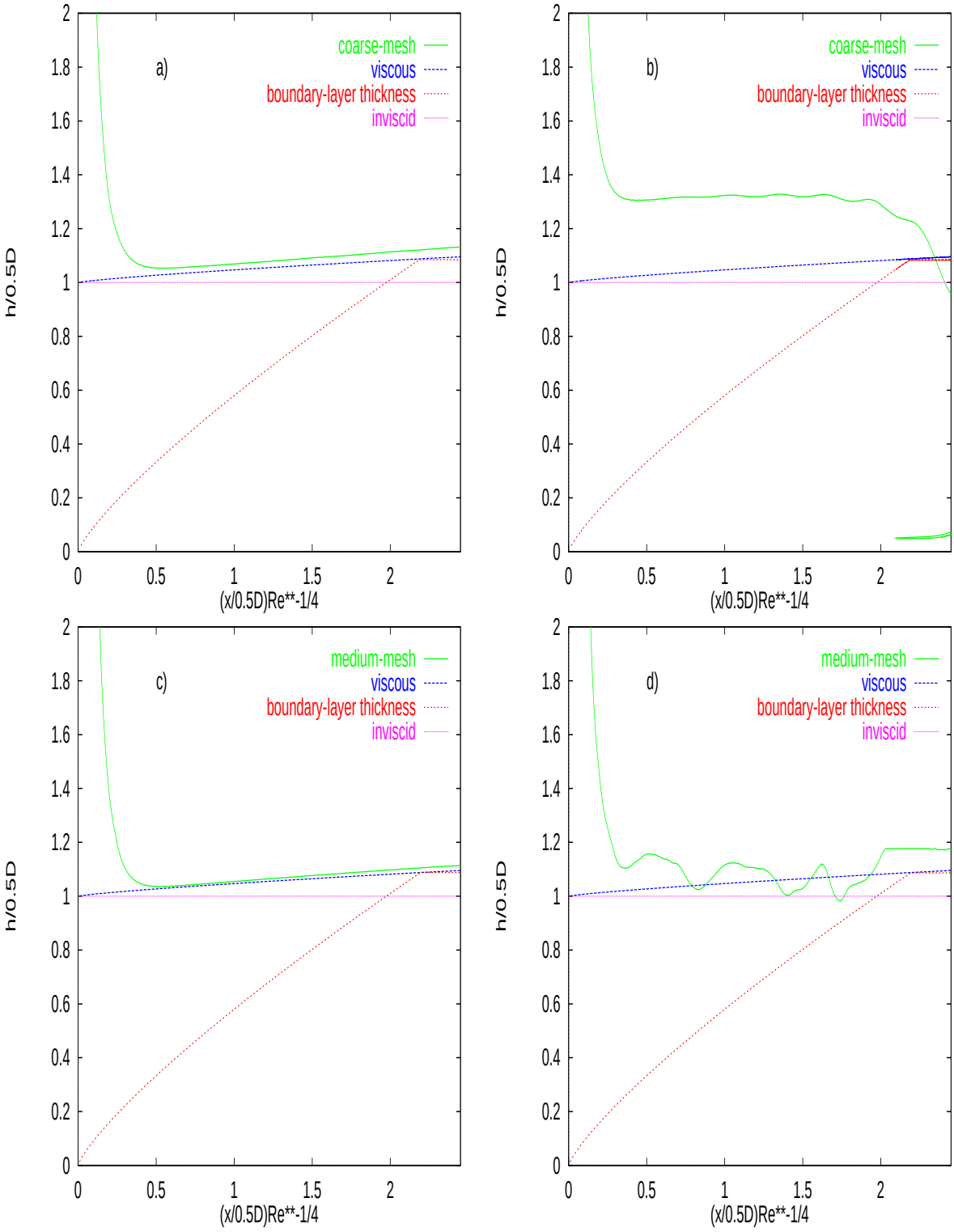

Figure 2: Comparison between the numerical solutions by using the $HRe\ \kappa-\varepsilon$ (left column) and $LRe\ \kappa-\varepsilon$ (right column) models and approximate analytic solutions by Watson.

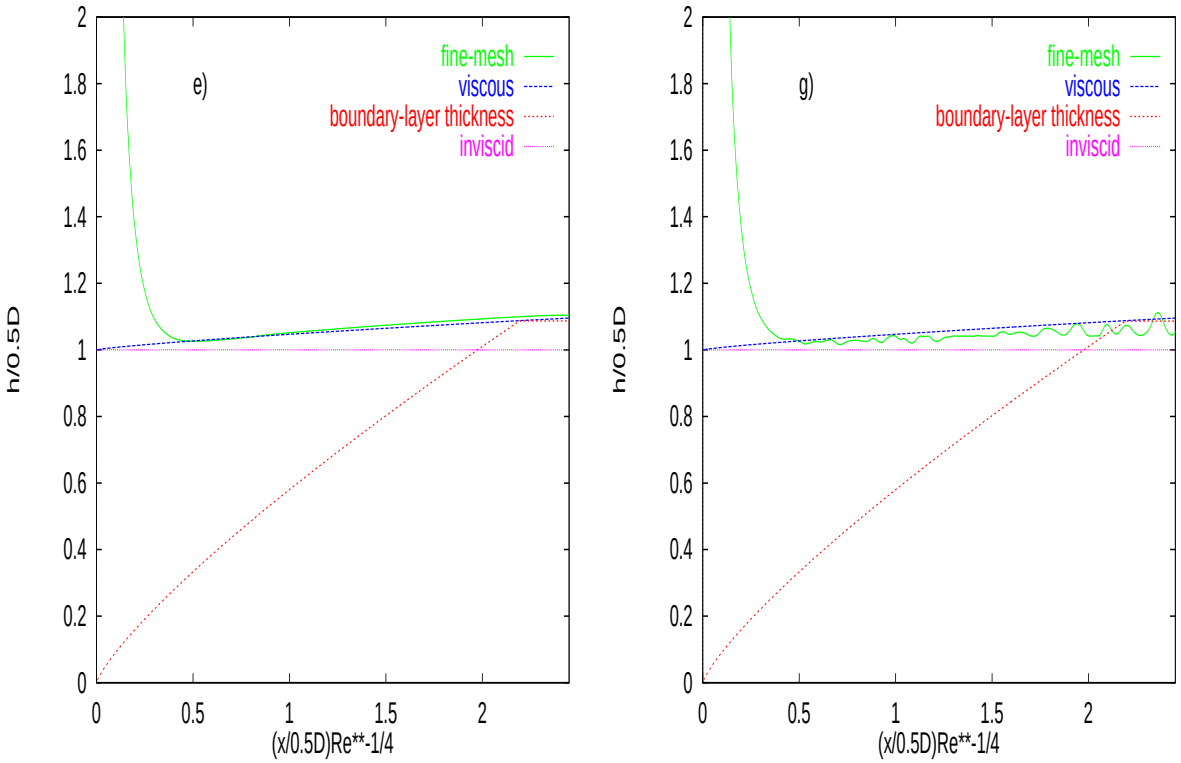

Figure 2: Continued

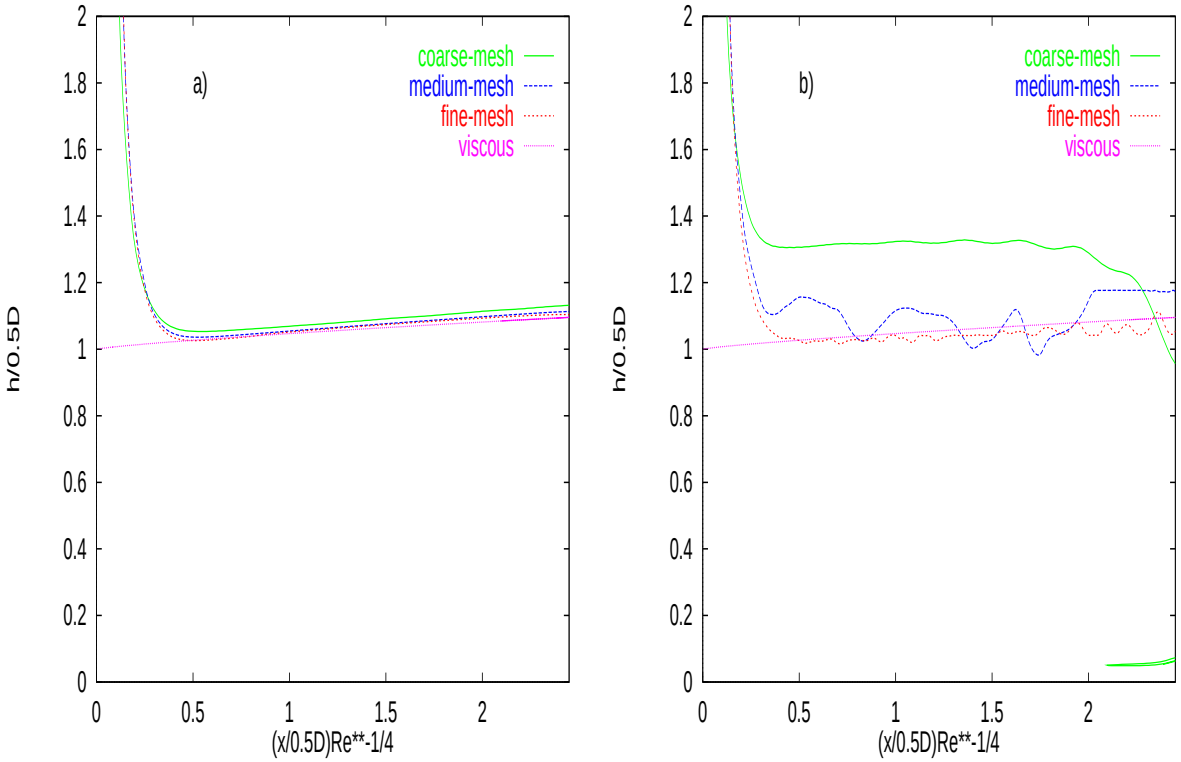

Figure 3: Comparison between of the three numerical solutions and viscous solution of Watson: a) $HRe\ \kappa - \varepsilon$ model; b) $LRe\ \kappa - \varepsilon$ model.

for $Re_x \leq 1.0 \times 10^6$, the discrepancy may be due to the uniform meshes used and the initial velocity profile not being sufficiently turbulent at the entrance region. Of course, near to $Re_x = 1.0 \times 10^6$, it may be noticed the tendency of the numerical profile, in the fine mesh (Fig. 1 c)), to follow the theoretical profiles.

Next, results with both the $HRe\ \kappa - \varepsilon$ and $LRe\ \kappa - \varepsilon$ models will be examined for a two-dimensional jet impinging onto a flat surface. For this free-surface fluid flow problem, the Reynolds number based on the inflow velocity $U_0 = 2.0$ m/s and inflow diameter $D = 1.0 \times 10^{-2}$ m is $Re = 3.2 \times 10^4$, and the Froude number is $F_r = U_0/\sqrt{gD} = 6.39$. Three different meshes are also used for this flow, namely: a coarse mesh (25×50 computational cells, $\delta x = \delta y = 0.002$ m); a medium mesh (50×200 computational cells, $\delta x = \delta y = 0.001$ m); and a fine mesh (100×400 computational cells, $\delta x = \delta y = 0.0005$ m). Figure 2 shows a comparison between the variation of the adimensional free-surface height $h/0.5D$ with adimensional distance $(x/0.5D)Re^{-1/4}$, obtained from the $HRe\ \kappa - \varepsilon$ (Figs. 2 a), c) and e) - left column) and $LRe\ \kappa - \varepsilon$ (Figs. 2 b), d) and g) - right column) models in the three meshes and at the adimensional time $t = 19.0$, and approximate viscous and inviscid solutions by Watson, 1964. In this picture, for simple information, Watson's boundary-layer thickness is also presented. It can be seen, from Figs. 2 (left column) and 3 a), that the calculations using the $HRe\ \kappa - \varepsilon$ model on fine mesh (200×400 nodes) provide, practically, the same results as the ones in the coarse and medium meshes, indicating grid independence of the numerical results. One can note also that the numerical results on coarse and medium meshes monotonicaly converge to the numerical solution on the fine mesh, and that the numerical solution on the fine mesh is in good agreement with the Watson's viscous solution.

At the same adimensional time of the simulation with the $HRe\ \kappa - \varepsilon$ model, the comparison between the free-surface height obtained from the $LRe\ \kappa - \varepsilon$ model and the Watson's viscous solution was also made, and the results are displayed in the Figs. 2 (right column) and 3 b). It is clear that the numerical results with this $\kappa - \varepsilon$ turbulence model on the three meshes are unsatisfactory. We believe that, for this especific fluid flow problem, the disagreement between viscous analytical solution, developed by Watson, and the numerical solution, obtained by the $LRe\ \kappa - \varepsilon$ model, may be attributed to the fact that the numerical solution has been calculated on a uniform mesh, resulting in a poor resolution of the viscous sublayer. In fact, for this Reynolds number flow dynamics, the thickness of the viscous sublayer of the turbulent boundary layer is so thin ($O(\nu/u_\tau)$, Gyr et al., 1999) that it would be difficult to resolve it in any reasonable time.

In terms of computational cost, it is important to note that when the $\kappa - \varepsilon$ turbulence model was applied with wall functions the computer cost was reduced by approximately a factor of 3.

6. Conclusion

Numerical simulations of turbulent fluid flow problems by using two versions of the $\kappa - \varepsilon$ models have been presented. In order to describe the turbulent effects on the averaged flow, the κ and ε conservation equations were analysed and implemented into the two-dimensional GENSMAC code.

In an attempt to obtain bounded transient solutions, the convection VONOS scheme was adopted for all non-linear derivatives of the convective transport equations. The numerical results show that it is not only beneficial, but also essential to incorporate this high-order oscillation-free upwinding method in order to reduce the effects of numerical diffusion in turbulent flow problems.

Particularly, the $HRe\ \kappa - \varepsilon$ model yields favorable predictions of zero-pressure-gradient turbulent boundary-layer on a flat plate (a confined flow) and a jet impinging onto a flat surface (a free-surface flow). On the other hand, the numerical results for these fluid flows using the $LRe\ \kappa - \varepsilon$ model were unsatisfactoy.

The simulations of the fluid flow problems presented in this paper confirm the importance of correctly prescribing the boundary conditions at the rigid-wall boundaries.

At the present, the authors are looking at the adaptation of these numerical techniques to more difficult fluid flow problems, such as those involving three dimensions.

7. Acknowledgments

We gratefully acknowledge the support given by FAPESP and DEMAC/IGCE/UNESP-Rio Claro.

8. References

Bradshaw, P., 1976, "Turbulence", Ed. Springer-Verlag, Germany, Topics in Applied Physics V. 12.

Durbin, P. A., 1996, On the $\kappa - \varepsilon$ Stagnation Point Anomaly, "Journal of Heat and Fluid Flow", Vol. 17, pp. 89–90.

Ferreira, V. G., 2001, "Análise e Implementação de Esquemas de Convecção e Modelos de Turbulência para Simulação de Escoamentos Incompressíveis Envolvendo Superfícies Livres", PhD thesis, ICMC-USP, São Carlos, Brazil.

Ferreira, V. G., Tomé, M. F., Mangiavacchi, N., Castelo, A., Cuminato, J. A., Fortuna, A. O., and McKee, S., 2002, High Order Upwinding and the Hydraulic Jump, "International Journal for Numerical Methods in Fluids", Vol. 39, pp. 549–583.

Gaskell, P. H. and Lau, A. K. C., 1988, Curvature-Compensated Convective Transport: SMART, A New Boundedness-Preserving Transport Algorithm, "International Journal for Numerical Methods in Fluids", Vol. 8, pp. 617–641.

Gyr, A., Kinzelbach, W., and Tsinober, A., 1999, "Fundamental Problematic Issues in Turbulence (*Trends in Mathematics*)", Ed. Birkhauser Verlag, Switzerland, Germany.

Hoffman, G., 1975, Improved Form of the Low Reynolds Number $\kappa - \varepsilon$ Turbulence Model, "The Physics of Fluids", Vol. 18, pp. 309–312.

Ladau, L. D. and Lifshitz, E. M., 1987, "Fluid Mechanics", Ed. Butterworth-Heinemann, 2^o Ed., Great Britain, Course of Theoretical Plysics V. 6.

Launder, B. E. and Spalding, D. B., 1974, The Numerical Computation of Turbulent Flows, "International Journal for Numerical Methods in Fluids", Vol. 15, pp. 127–146.

Norris, H. L. and Reynolds, W. C., 1975, Turbulent Channel Flow with a Moving Wavy Boundary, Stanford Univ. Dept. Mech. Eng.,TR TF-7.

Sondak, D. L. and Pletcher, R. H., 1995, Application of Wall Functions to Generalized Nonorthogonal Curvilinear Coordinate Systems, "AIAA Journal", Vol. 33, pp. 33–41.

Tomé, M. F., Castelo, A., Murakami, J., Cuminato, J. A., Minghim, R., Oliveira, C. F., N, M., and McKee, S., 2000, Numerical Simulation of Axisymmetric Free Surface Flows, "Journal of Computational Physics", Vol. 157, pp. 441–472.

Tomé, M. F. and McKee, S., 1994, GENSMAC: A Computational Marker-and-Cell Method for Free Surface Flows in General Domains, "Journal of Computational Physics", Vol. 33, pp. 171–186.

Varonos, A. and Bergeles, G., 1998, Development and Assessment of a Variable-Order Non-Oscillatory Scheme for Convection Term Discretization, "International Journal for Numerical Methods in Fluids", Vol. 26, pp. 1–16.

Watson, E. J., 1964, The Radial Spread of a Liquid Jet over a Horizontal Plane, "Journal of Fluid Mechanics", Vol. 20, pp. 481–499.

White, F. M., 1991, "Viscous Fluid Flow", Ed. McGraw-Hill, Inc., 2^o Ed., New York, USA.

Wilcox, D. C., 1988, Reassessment of the Scale-Determining Equation for Advanced Turbulence Models, "AIAA Journal", Vol. 26, pp. 1299–1310.

Yang, Z. and Shih, H., 1993, New Time Scale Based $\kappa - \varepsilon$ Model for Near-Wall Turbulence, "AIAA Journal", Vol. 7, pp. 1191–1198.